Preferential binding between intracellular organic matters and Al$_{13}$ polymer to enhance coagulation performance

Ruiping Liu[1,2], Tingting Guo[1,3], Min Ma[1,4], Mingquan Yan[5], Jing Qi[1], Chengzhi Hu[1,2,*], Gang Liu[6], Huijuan Liu[2,7], Jiuhui Qu[1,2], Walter van der Meer[8]

1. Key Laboratory of Drinking Water Science and Technology, Research Center for Eco-Environmental Sciences, Chinese Academy of Sciences, Beijing 100085, China
2. University of Chinese Academy of Sciences, Beijing 100049, China
3. Beijing University of Technology, Beijing 100124, China
4. Beijing Waterworks Group, Beijing 100031, China
5. Department of Environmental Engineering, Peking University, Beijing 100871, China
6. Sanitary Engineering, Department of Water Management, Faculty of Civil Engineering and Geosciences, Delft University of Technology, 2600GA Delft, the Netherlands
7. State Key Laboratory of Environmental Aquatic Chemistry, Research Center for Eco-Environmental Sciences, Chinese Academy of Sciences, Beijing 100085, China
8. Science and Technology, University of Twente, 7500AE Enschede, the Netherlands

ARTICLE INFO

ABSTRACT

Coagulation is the best available method for removing intracellular organic matter (IOM), which is released from algae cells and is an important precursor to disinfection by-products in drinking water treatment. To gain insight into the best strategy to optimize IOM removal, the coagulation performance of two Al salts, i.e., aluminum chloride (AlCl$_3$) and polyaluminum chloride (PACl, containing 81.2% Al$_{13}$), was investigated to illuminate the effect of Al species distribution on IOM removal. PACl showed better removal efficiency than AlCl$_3$ with regard to the removal of turbidity and dissolved organic carbon (DOC), owing to the higher charge neutralization effect and greater stability of pre-formed Al$_{13}$ species. High pressure size exclusion chromatography analysis indicated that the superiority of PACl in DOC removal could be ascribed to the higher binding affinity between Al$_{13}$ polymer and the low and medium molecular weight (MW) fractions of IOM. The results of differential log-transformed absorbance at 254 and 350 nm indicated more significant formation of complexes between AlCl$_3$ and IOM, which benefits the removal of tryptophan-like proteins thereafter. Additionally, PACl showed more significant superiority compared to AlCl$_3$ in the removal of <5 kDa and hydrophilic fractions, which are widely viewed as the most difficult to remove by coagulation. This study provides insight into the interactions between Al species and IOM, and advances the optimization of coagulation for the removal of IOM in eutrophic water.

© 2018 The Research Center for Eco-Environmental Sciences, Chinese Academy of Sciences.
Published by Elsevier B.V.

* Corresponding author. E-mail: czhu@rcees.ac.cn (Chengzhi Hu).

Introduction

Excessive discharge of nitrogen and phosphorus accelerates the eutrophication of lakes and reservoirs, and the widespread algae blooms thereafter. This problematic algae bloom in water sources interferes with drinking water treatment processes such as coagulation (Cheng and Chi, 2003; Takaara et al., 2010), sedimentation (Aktas et al., 2013), medium filtration (Ewerts et al., 2014), and membrane filtration (Elcik et al., 2016). Additionally, algogenic organic matter (AOM) always accompanies cyanobacteria cells, and is typically related to problems with toxins (Zamyadi et al., 2012), taste and odor (Watson et al., 2016), and assimilable organic carbon (AOC) (Hammes et al., 2007), and the formation of disinfection by-products (DBPs) (Fang et al., 2010; Song et al., 2016). The components and characteristics of AOM are highly dependent on the algae species and their growth stage (Henderson et al., 2008), and their DBP formation is rather different and dependent on molecular weight and hydrophilicity (Fang et al., 2010). Additionally, AOM is usually referred to as intracellular organic matter (IOM) and extracellular organic matter (EOM), with distinct components and characters. Typically, AOM mainly includes bio-chemicals such as metabolites, nucleic acids (DNA and RNA) (Hammes et al., 2007), proteins, peptides, amino acids, polysaccharides, oligosaccharides, and traces of other organic acids such as humic-like substances (Pivokonsky et al., 2006; Henderson et al., 2008). IOM mainly exists in algae cells and has higher concentration than EOM, and the removal of algae cells may achieve promising IOM removal. On the basis of this consideration, the removal of IOM may not be problematic if algae suspensions are well removed. However, the inactivation of algae cells by pre-oxidation inevitably causes IOM release, which occurs upon exposure of algae cells to oxidants such as chlorine, ozone, and permanganate (Hoyer et al., 1987; Hammes et al., 2007; Chen et al., 2009; Ma et al., 2012a). It has been demonstrated that IOM is an important precursor to the formation of disinfection by-products. In considering the widely-used preoxidation methods, the satisfactory removal of released IOM prior to post-chlorination is of crucial importance to minimize its adverse effects on drinking water safety.

IOM exhibits significantly different characteristics from natural organic matter (NOM) in terms of charge density, hydrophobicity, and molecular weight distribution (Henderson et al., 2008), and the conventional strategies to remove NOM may show different performances towards IOM. To promote a feasible process for IOM removal, the characteristics of the different components and their removal behaviors should be well investigated. The hydrophilic organic matters accounted for 86% and 63% of dissolved organic carbon (DOC) in cell organic matter (COM) and EOM, respectively. The molecular weight (MW) fractions of COM below 800 kDa comprised 69% of DOC, whereas EOM primarily contained 1–100 kDa molecules (Li et al., 2012). Additionally, AOM behaves similarly to non-ionic polymers or anionic polyelectrolytes (Bernhardt et al., 1985; Hoyer et al., 1987; Paralkar and Edzwald, 1996; Pivokonsky et al., 2006), and its effects on water treatment, especially coagulation (Bernhardt et al., 1985; Hoyer et al., 1987; Paralkar and Edzwald, 1996; Chen et al., 2009), ultrafiltration (Qu et al., 2012), and nanofiltration (Her et al., 2004), have been extensively investigated. On the one hand, AOM at low levels has been reported to aid coagulation *via* bridging effects and to improve the adhesion efficiency of particles (Pivokonsky et al., 2006; Ma et al., 2012b; Gonzalez-Torres et al., 2014). However, AOM at undesirably high concentrations consumes coagulants and decreases the surface charge of particles, and adversely inhibits coagulation and filtration thereafter (Chen et al., 2009; Ma et al., 2012b). It was reported that the peptides and proteins within AOM tend to form complexes with metal ions (Baresova et al., 2015), and this effect consumes coagulants and decreases the amount of coagulants available for charge neutralization. Besides the effects of AOM concentrations, the AOM components with different characteristics also showed remarkably different effects on coagulation. For example, the COM contains a large number of proteins with high affinity towards polyaluminum chloride (PACl), and consequently exhibits much stronger inhibitive effects on the flocculation of suspended kaolin than EOM does (Takaara et al., 2007).

AOM species with different MW fractions and polarity may show remarkably different behavior during the coagulation process, and their treatability by coagulation is also assumed to be rather distinct. Upon their release from algae cells, coagulation may be the most effective and best available method to enhance IOM removal among the conventional water treatment processes. The Al-based coagulants, such as PACl and aluminum sulfate (alum), show different coagulation mechanisms and efficiency depending on water quality, especially as regards the properties of organics (Duan et al., 2014; Tang et al., 2015). PACl, with high content of preformed Al_{13} species, shows higher charge density and stronger bridging ability, and has been widely believed to be superior in terms of floc growth (Tang et al., 2015), DOC removal (Duan et al., 2014), and filterability (Jiao et al., 2016). However, our previous study indicated better performance for $AlCl_3$, as compared to PACl, in the treatment of eutrophic water with high alkalinity, owing to the *in situ* formed Al_{13} and the beneficial pH control effect during $AlCl_3$ coagulation (Hu et al., 2006). Al salts with different Al species distribution also showed different removal efficiencies towards disinfection byproduct precursors from NOM with different components (Zhao et al., 2008). Unfortunately, studies on the removal of IOM with different molecular characteristics by coagulation are relatively rare to the best of our knowledge. The interactions between different IOM components and Al species fractions are far from well-illustrated, the understanding of which may provide insight for the optimization and enhancement of IOM removal from drinking water.

On the basis of these considerations, this study aims to systematically investigate the coagulation efficiency of $AlCl_3$ and PACl (81.2% Al_{13}) in a wide Al dose range towards IOM extracted from *M. aeruginosa* suspensions. Additionally, the obtained IOM were respectively fractioned into different fractions with different MW, distribution and hydrophilicity, and particular emphasis was paid to the preferential binding between these IOM fractions and Al species. These results may be of practical value to enhance IOM removal and to control its adverse effects on DBP formation in the treatment of algae bloom source waters.

1. Materials and methods

1.1. *M. aeruginosa* cultivation and intracellular organic matter (IOM) extraction

The axenic strain of *M. aeruginosa* (No. FACHB-905) was obtained from Wuhan Institute of Hydrobiology, Chinese Academy of Sciences, and was then cultured in a biological incubator with a cycle of 14-hr light and 10-hr dark at 25°C. The detailed methods were described in our previous study (Ma et al., 2012a).

After cultivation for 16 days, the *M. aeruginosa* cell growth was in the steady-state stage and was used for AOM extraction following the following procedures. First, *M. aeruginosa* cells were collected by 30-min centrifugation at 6000 r/min, and the obtained algae suspension was resuspended in Milli-Q water and centrifuged at 6000 r/min for 20 min. After that, the obtained cells were sonicated for 60 min and re-suspended in 20-mL Milli-Q water. The suspension was stored at −80°C to destroy the algae cells in order to achieve the release of IOM without surface retained organic matter (SOM) as much as possible. After being thawed at room temperature, the sample was filtered through a 0.22-μm membrane filter and the organic matter in the filtrate was referred to as IOM. After removing the suspended algae remains, the filtrate appeared green and the absorbance at 680 nm, as expressed by A_{680}, was indicative of the presence of pigment-like organics such as chlorophylls and carotenoids (Becker, 1994).

1.2. Chemicals and reagents

Aluminum chloride hexahydrate ($AlCl_3 \cdot 6H_2O$, GR) was purchased from Beijing Chemical Reagent Co., Ltd., China, and PACl with basicity of 2.2 was prepared by an electrolysis method as reported in our previous study (Hu et al., 2006). The Al species (Al_a, Al_b, and Al_c) distribution was measured by the Al Ferron method, and the detailed analysis procedure can be found in the literature (Hu et al., 2006; Yan et al., 2013). The ratios of Al_a, Al_b, and Al_c within $AlCl_3$ were determined to be 94.4%, 5.6%, and 0%, whereas those within PACl were 12.0%, 80.1%, and 8.9% accordingly. Unless otherwise noted, the other chemicals used in this study were of analytical grade.

1.3. IOM fractionation

To obtain IOM fractions with different MW and hydrophobicity, the IOMs were respectively separated by ultrafiltration membranes and resins, and the concentrations of DOC in these samples were analyzed. The difference between the summative DOC and that prior to fractionation was below 5%.

1.3.1. Fractionation by ultrafiltration
According to the methods described in our previous study (Zhao et al., 2008), the diluted IOM at 20 mg/L as DOC was fractionated into four fractions of <5 kDa, 5–30 kDa, 30–100 kDa, and >100 kDa using a stirred ultrafiltration cell device (Model 8200, Amicon, Millipore) by cellulose membranes (PL, 63.5 mm, Millipore) with different nominal molecular weight cutoffs. The obtained samples were stored in 4°C in TEFLON (PTFE) sealed glass vessels. To obtain stock solutions of different IOM fractions, similar procedures were used except that the undiluted IOM solution was used.

1.3.2. Fractionation by resins
To obtain fractions with different hydrophobicity, *i.e.*, hydrophilic (HPI), transphilic (TPI), and hydrophobic (HPO), methods described in a previous study were used (Henderson et al., 2008). Briefly, the IOM solution with 20 mg/L DOC was acidified to pH 2 and passed through Amberlite XAD-4 and XAD-8 (60–80 mesh) resins in series. After that, these two resin columns were respectively back-eluted with 0.1 mol/L NaOH. The organics in the non-retained effluent were referred to as HPI, whereas those in the XAD-8 and XAD-4 resin back-effluents were expressed as HPO and TPI, respectively.

1.4. Experimental methods

The raw water was prepared by the addition of IOM, Kaolin suspension (23,000–02, Kanto, Tokyo, Japan), sodium bicarbonate ($NaHCO_3$) as alkalinity, and potassium chloride (KCl) as background electrolytes into Milli-Q water. The main parameters in the prepared water were as follows: DOC = 8.1 ± 0.3 mg/L, turbidity = 100 nephelometric turbidity units (NTU), alkalinity = 100 mg/L as $CaCO_3$, and KCl = 3.3 mmol/L. pH was adjusted by sodium hydroxide (NaOH, GR) and hydrochloric acid (HCl, GR) to 7.0 ± 0.1. While investigating the removal of different IOM fractions, similar procedures were used except that the IOM fractions were dosed and DOC was controlled at 5.0 ± 0.2 mg/L.

Coagulation tests were performed with 500 mL samples in 800-mL beakers and conducted on a programmable jar tester (MY3000–6, MeiYu, China). After dosing coagulants during the initial 20-sec rapid mixing stage at 250 r/min, the samples were rapidly mixed at 200 r/min for 2 min and then slowly mixed at 40 r/min for 15 min, consecutively. After 30-min sedimentation, the supernatants (200 mL) were carefully collected to avoid entrainment of the precipitated solids. Turbidity was directly analyzed without any pretreatment. DOC, the absorbance at 254 nm (UV_{254}) and 680 nm (A_{680}), and the excitation-emission matrix (EEM) fluorescence spectra of the collected supernatants were analyzed after being filtered through 0.45-μm membranes.

To illustrate the interactions between IOM and these two Al species, PACl and $AlCl_3$, in the Al dose range from 0.05 to 0.5 mg/L as Al, were respectively dosed into IOM solution (DOC = 8.1 ± 0.3 mg/L) without the addition of kaolin suspension. After 5-sec rapid mixing (250 r/min) and 2-min reaction (40 r/min), the samples were collected and the UV_{254} and the absorbance at 350 nm (A_{350}) were directly analyzed by a spectrophotometer without either sedimentation or membrane filtration. The values of differential log-transformed absorbance at 254 nm ($DLnA_{254}$) and that at 350 nm ($DLnA_{350}$) were calculated according to the methods proposed by Yan et al. (2013. (Appendix A Text S1)

1.5. Analysis methods

Solution pH was analyzed by a 720A pH meter (Thermo Orion, USA). Turbidity was measured by a HACH2100N turbidimeter. The A_{680}, UV_{254}, and A_{350} values were measured by a U-3010 Spectrophotometer (Hitachi Co., Japan) in a 1-cm quartz cell,

and the DOC concentrations were determined by a TOC-VCPH total organic carbon analyzer (Pheonix8000, TeKmar-Dohrmann, USA).

The fluorescence excitation-emission matrices (EEMs) of supernatants were recorded on an F-2500 spectrofluorometer (Hitachi Co., Japan) by scanning emission spectra as a function of excitation wavelength. An excitation wavelength from 200 to 400 nm in 5 nm steps was used, and emission wavelengths from 290 to 550 nm in 5 nm steps were measured. Milli-Q water was used as a blank sample. The method as reported by Chen et al. (2003) was used to integrate the area beneath EEM spectra (appendix A Text S2). The fluorescence index (FI) is indicative of the ratios of intensities at λ_{em} of 450 nm to that at 500 nm (λ_{ex} = 370 nm), and it is reported to be correlated to the aromaticity and protein content within organics (Cory et al., 2010).

High pressure size exclusion chromatography (HPSEC) was utilized to investigate the molecular size distribution of different IOM fractions after coagulation with elevated Al doses. HPSEC was performed at room temperature with an Agilent 1260 Infinity with UV/Vis detector, and the experimental details have been described elsewhere (Chow et al., 2008).

2. Results and discussion

2.1. Coagulation behaviors of AlCl$_3$ and PACl towards IOM

2.1.1. Turbidity removal and residual Al
Fig. 1a compares the turbidity removal efficiency between AlCl$_3$ and PACl with elevated Al doses from 0.5 to 7.0 mg/L. In the presence of IOM, the kaolin suspension showed ζ-potential of as low as −47.2 mV, and PACl contributed to lower turbidity than AlCl$_3$ over a wide Al dose range. Generally three stages were observed in terms of turbidity removal with elevated Al doses. In the first stage, turbidity removal was positively correlated with higher Al doses at Al < 2 mg/L. After that, the turbidity removal was stable and above 95% for Al doses of 2.0–6.0 mg/L. The extremely high Al dose of 7.0 mg/L significantly inhibited turbidity removal, with values as low as 31.5% and 47.0% for AlCl$_3$ and PACl, respectively. PACl exhibited more significant efficacy for charge neutralization than AlCl$_3$, and the ζ-potential approached 0 mV at lower Al doses (Appendix A Fig. S1). AlCl$_3$ at 2 mg/L as Al increased the ζ-potential to −20.2 mV whereas PACl contributed to a significant increase to −5.6 mV. At the high Al dose of 7 mg/L, the formed flocs re-stabilized due to the high reversed ζ-potential, and increased turbidity was observed accordingly.

Besides the charge neutralization effects, the hydrolysis and precipitation of Al salts also played an important role in the observed coagulation behaviors. In the Al range from 0.5 to 2.0 mg/L, the residual Al decreased with elevated Al doses, with the lowest values of 0.13 and 0.06 mg/L for AlCl$_3$ and PACl (Fig. 1b) respectively. After that, further increases in Al doses contributed to higher residual Al, and at 7 mg Al/L the residual Al achieved the maximum concentrations of 0.59 and 0.28 mg Al/L for AlCl$_3$ and PACl, respectively. Interactions between IOM and Al, i.e., the formation of soluble Al-IOM complexes, occurred and affected the coagulation behaviors. In the insufficient Al dose range, Al-IOM complexation
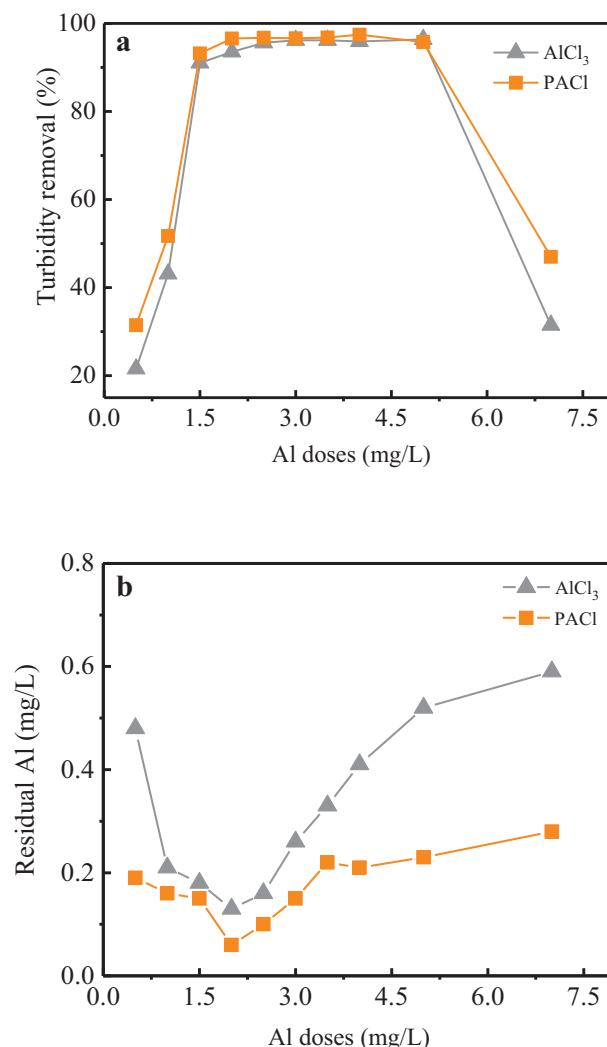

Fig. 1 – Comparison of polyaluminum chloride (PACL) and AlCl$_3$ in terms of (a) turbidity removal and (b) residual soluble Al after 15-min sedimentation. DOC = 8.1 mg/L, Turbidity = 100 nephelometric turbidity units (NTU), Initial pH = 7.0.

inhibited Al hydrolysis and decreased the amount of Al salts available for charge destabilization, and hindered coagulation thereafter. This assumption was supported by the high residual Al observed (Fig. 1b). In the sufficient Al dose range, with high ratios of Al to IOM ($R_{Al:IOM}$), the consumption of Al salts by IOM may be neglected. At the extremely high Al dose of 7 mg/L, the reversal of the ζ-potential hindered the aggregation of destabilized colloids. Additionally, the hydrolysis of AlCl$_3$ consumed more alkalinity, and the more significant pH decrease (Appendix A Fig. S2) may also contribute to higher levels of residual Al.

2.1.2. Removal of DOC, UV$_{254}$, and A$_{680}$
PACl contributed to more significant DOC removal than AlCl$_3$ over a wide range of Al doses, from 0.5 to 7.0 mg/L (Fig. 2a). At a dose of less than 1 mg/L, the DOC removal was respectively observed to be 38.0% by PACl and 17.9% by AlCl$_3$, and the maximum DOC removal was determined to be 67.5% by PACl at 3.5 mg/L and 61.4% by AlCl$_3$ at 4.0 mg/L accordingly. IOMs
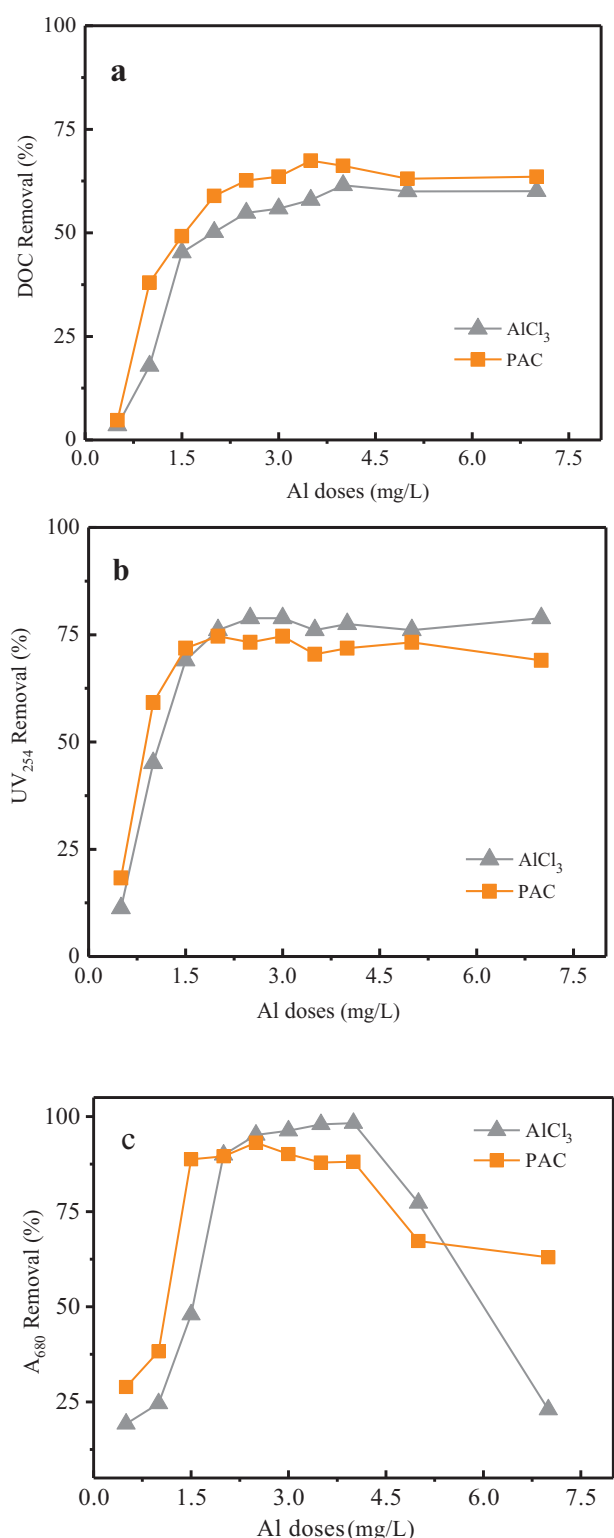
Fig. 2 – Comparison of PACl and AlCl$_3$ coagulation efficiency in terms of the removal of DOC, UV$_{254}$, and A$_{680}$ after 15-min sedimentation and 0.45-μm membrane filtration. DOC = 8.1 mg/L, Turbidity = 100 nephelometric turbidity units (NTU), Initial pH = 7.0.

are composed of different organic species such as proteins, polysaccharides, and metabolites with different characteristics (Pivokonsky et al., 2006; Henderson et al., 2008), and Al

coagulants may show different coagulation behaviors towards them. To illustrate this assumption, the removals of pigment-like organics (expressed as A$_{680}$) and the unsaturated organics (expressed as UV$_{254}$) were compared (Fig. 2b and c). At Al < 2 mg/L, PACl achieved more significant removal of A$_{680}$ and UV$_{254}$, but AlCl$_3$ contributed to lower residual values of A$_{680}$ and UV$_{254}$ at higher Al doses above 3 mg/L.

The higher efficiency of A$_{680}$ and UV$_{254}$ removal by AlCl$_3$ might be attributed either to the lower concentrations of pigment-like and unsaturated organics or to the adverse effects on A$_{680}$ and UV$_{254}$ analysis that were induced by the lower pH after flocculation. AlCl$_3$ hydrolysis consumed more alkalinity than PACl, and the equilibrium pH after AlCl$_3$ coagulation was lower (Appendix A Fig. S2). However, IOM showed little variation in terms of UV–Vis absorption spectra over a wide pH range from 4.0 to 8.5 (Appendix A Fig. S3). Consequently, the pH effect on the analysis of A$_{680}$ and UV$_{254}$ was rather weak and can be ignored. On the other hand, the formation of complexes between metal ions (Me) and organics such as IOM can impact the absorbance of NOM at 254 nm (Yan et al., 2013), and this effect may also interfere with the UV$_{254}$ analysis. To quantify this effect on UV–Vis absorbance, AlCl$_3$ and PACl at doses near the soluble Al concentrations in Fig. 1b, i.e., 0.05 to 0.5 mg/L, were respectively introduced into IOM solution, and the UV–Vis absorption spectra were directly measured without filtration. The results shown in Appendix A Fig. S4 indicated that the introduction of AlCl$_3$ contributed to a steady UV$_{254}$ increase from 0.128 to 0.169 cm^{-1}. PACl at 0.05–0.1 mg/L also contributed to UV$_{254}$ increase from 0.171 to 0.191 cm^{-1}, and further elevated PACl doses decreased rather than increasing UV$_{254}$. The formation of Al-IOM complexes did have an influence on UV$_{254}$ absorbance (Yan et al., 2013), and the different Al species may show different complexation behaviors towards IOM. The residual Al levels in AlCl$_3$ coagulation were higher than those in PACl coagulation (Fig. 1b), and more remarkable UV$_{254}$ increase due to Al-IOM complexation was assumed to occur. On the basis of this consideration, the higher removal of A$_{680}$ and UV$_{254}$ in the Al dose range above 3.0 mg/L, as observed in Fig. 2, was attributed to the more significant efficacy of AlCl$_3$ at removing the pigment-like and unsaturated IOM.

Additionally, it was observed that A$_{680}$ removal started to decrease in the Al dose range above 4 mg/L for the two coagulants (Fig. 2c), whereas UV$_{254}$ removal barely decreased, even at the extremely high Al dose of 7 mg/L (Fig. 2b). The different MW IOM components contributing to UV$_{254}$ and A$_{680}$ were analyzed, and results are illustrated in Table 1. It was observed that the high MW IOM, i.e., the >100 kDa fraction, contributed as high as 73.2% of the total absorbance of IOM at 680 nm. The pigment-like organics, such as the chlorophyll and carotenoid contents, are important components within algae cells, the content of which is in the range from 0.1 to 9.7% of the wet biomass (Nicholls and Dillon, 1978). Table 1 indicates that A$_{680}$ corresponded to the high MW IOM and may be viewed as organic colloids, and the overdosing with Al contributed to their restabilization and dissolution. A$_{680}$ removal by sedimentation showed similar trends to that of the filtrate from a 0.45-μm membrane (Appendix A Fig. S5), and this supported the dissolution of destabilized IOM into solution. The charge neutralization effect was inferred to play an important role in A$_{680}$ removal by Al coagulation. Comparatively, the removal of UV$_{254}$ species with lower MW was

Table 1 – Molecular weight distribution of intracellular organic matter by ultrafiltration fractionation.

MW (kDa)	DOC (mg/L) (%)	UV$_{254}$* (cm^{-1})	SUVA$_{254}$ (L/(mg·m))	A$_{680}$[a] (cm^{-1})	FI	EEM Intensity[b] (A.U.)			
						Peak P1	Peak P2	Peak H	Peak DM
>100	7.09(34.9)	0.23	3.24	0.041	4.23	/	594.2	34.3	/
30–100	4.46(21.9)	0.17	3.81	0.010	5.65	/	398.2	98.1	/
5–30	4.84(23.8)	0.15	3.10	0.004	6.02	/	204.9	95.5	/
<5	3.94(19.4)	0.20	5.21	0.001	6.78	329.3	479.9	56.6	68.6

Peak P2: Tryptophan-like, maxima at (219,340).
Peak H: Humic-like, maxima at (256,438).
Peak DM: Dissolved microbial metabolites, maxima at (262,338).
/: EEM intensity is less than 1.0.
[a] The samples were diluted prior to UV–Vis analysis to obtain the desired absorbance range.
[b] Peak P1: Tyrosine-like, maxima at (219,296).

mainly attributed to their being adsorbed onto Al precipitates and was barely affected by ζ-potential reversal. This result indicated that the various IOM components may be removed by different coagulation mechanisms, and their removal strategy should be carefully evaluated.

2.2. Removal of IOM fractions with different MW by Al coagulation

2.2.1. Characteristics of IOM with different MW

The extracted IOMs (20 mg/L as DOC) were fractioned by ultrafiltration membranes, and the values of DOC, UV$_{254}$, SUVA, and EEM Intensity for each fraction are illustrated in Table 1. The fractions with different MW ranges of <5 kDa, 5–30 kDa, 30–100 kDa, and >100 kDa showed DOC concentrations of 7.09, 4.46, 4.84, and 3.94 mg/L, which contributed 34.9%, 21.9%, 23.8%, and 19.4% to total DOC. The 30–100 kDa fraction showed higher SUVA$_{254}$ values than the 5–30 kDa fraction, although similar DOC levels between these two fractions were observed. IOM showed relatively low SUVA$_{254}$ values as compared to NOM-, indicating a dominance of low-aromaticity compounds with low UV$_{254}$ absorbance, such as hydrophobic proteins and hydrophilic polysaccharides (Edzwald, 1993). Additionally, the organics with specific absorbance at 680 nm as expressed by A$_{680}$ mainly existed in the fraction >100 kDa, with contribution of 73.2% to the total A$_{680}$, and this implied the feasibility of using coagulation to control algal color by removal of the A$_{680}$ fraction with high MW.

EEM is widely used to effectively characterize IOM fractions (Henderson et al., 2008) and as an index for the removal of organic matter by coagulation (Gone et al., 2009). The EEM fluorescence spectra of these fractions showed that IOM consisted of four fluorescence peaks, which can be designated as follows: tyrosine-like aromatic proteins (Peak P1), tryptophan-like aromatic proteins (Peak P2); dissolved microbial metabolites (Peak DM), and humic-like substances (Peaks H) (Chen et al., 2003) (Appendix A Fig. S6). Quantitatively, the tryptophan-like aromatic proteins outweighed the other species i.e., tyrosine-like, humic-like, and dissolved microbial metabolites, for these four IOM fractions with different MW. The intensity of tryptophan-like aromatic proteins in >100, 30–100, 5–30, and <5 kDa fractions was determined to be 594.2, 398.2, 204.9, and 479.9 A.U., respectively. The tyrosine-like and dissolved microbial metabolites mainly existed in the <5 kDa fraction.

In addition, the IOM fractions with higher MW were related to lower FI values (Ex = 370 nm, Em = 450/500 nm). The FI values have been reported to be positively correlated with the protein content within organics, so that the protein-rich IOM was inferred to mainly exist in the fraction with lower MW. The results of the EEM intensity analysis also supported the protein content (Peak P1 and P2) mainly existing in the <5 kDa fraction.

2.2.2. Removal of IOM fractions with different MW by Al coagulation

The HPSEC chromatograms of IOM mainly showed 7 peaks (Fig. 3), i.e., Peak 1 to Peak 7, and the peaks appearing at lower retention time (RT) were related to the higher MW fractions; meanwhile, with elevated Al doses from 0.5 to 7.0 mg/L, the numbers and the intensity of the peaks changed to some extent, especially for higher MW fractions. In particular, the two peaks (Peaks 1 and 2) were higher with the dose of Al 0.5 mg/L, however, both were lower when the dosing of Al was 1.5 mg/L. According to the methods developed by Matilainen et al. (2011), the weight-averaged MW of these peaks were determined to be 1,133,588, 33,447, 7324, 3555, 2447, 150, and 77 Da. Additionally, the chromatogram peaks of Peak 1 to 3 were classified as high-Mw (HMw) peaks, the two peaks of Peak 4 and 5 were referred to as moderate-Mw (MMw) peaks, and the peaks of Peak 6 and 7 were denoted as low-Mw (LMw) peaks. The weighted intensities of HMw, MMw, and LMw were calculated by Eqs. (1)–(3). The MMw was related to the IOM fractions with the highest absorption intensity at 254 nm, whereas LMw was indicative of those with the lowest absorbance among these IOM species.

$$\mathrm{HMw} = \sum_{i=1}^{3} h_i M_i \Big/ \sum_{i=1}^{3} M_i \tag{1}$$

$$\mathrm{MMw} = \sum_{i=4}^{5} h_i M_i \Big/ \sum_{i=4}^{5} M_i \tag{2}$$

$$\mathrm{LMw} = \sum_{i=6}^{7} h_i M_i \Big/ \sum_{i=6}^{7} M_i \tag{3}$$

where h_i and M_i are the height and molecular weight of peak "i".

For a more detailed description of the results from Fig. 3, the removal behaviors of HMw, MMw, and LMw fractions were
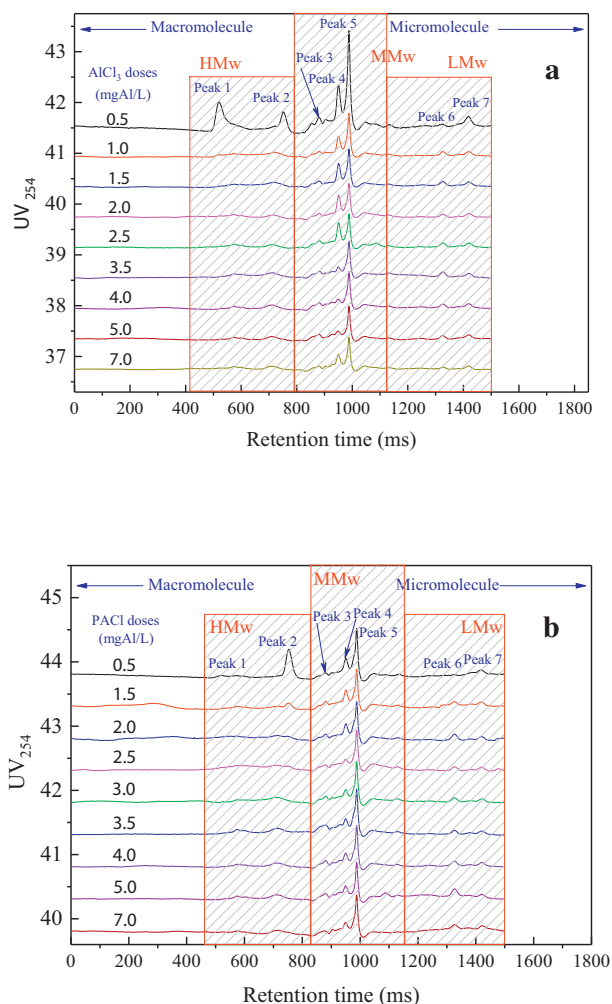
Fig. 3 – IOM HPSEC chromatogram transformation after coagulation by (a) AlCl₃ and (b) PACl with elevated Al doses from 0.5 to 7.0 mg/L. DOC = 8.1 mg/L, Turbidity = 100 nephelometric turbidity units (NTU), Initial pH = 7.0.
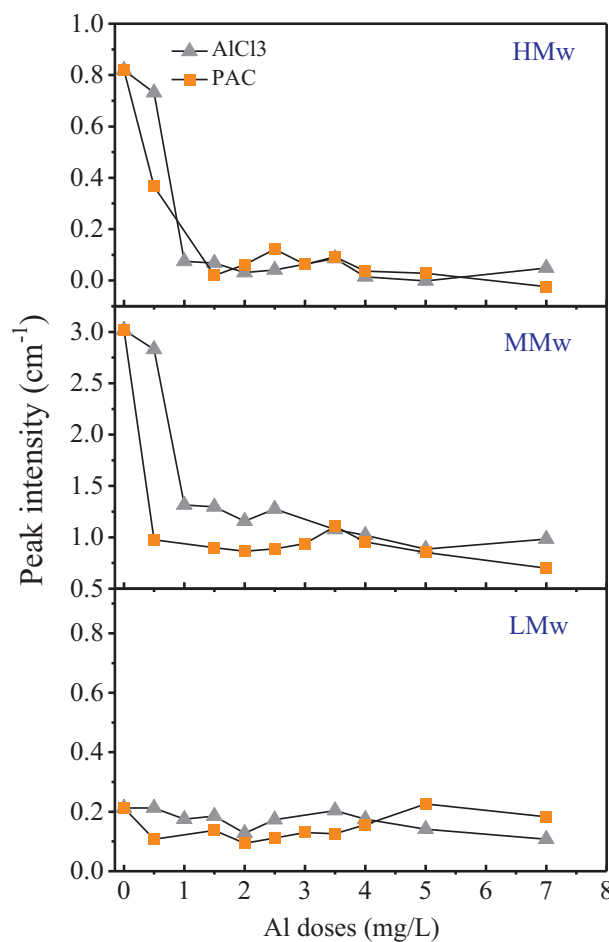

Fig. 4 – The removal behaviors of high molecular weight (HMw), moderate molecular weight (MMw), and low molecular weight (LMw) fractions after coagulation by AlCl₃ and PACl with elevated Al doses from 0.5 to 7.0 mg/L. DOC = 8.1 mg/L, Turbidity = 100 nephelometric turbidity units (NTU), Initial pH = 7.0.

investigated with AlCl₃ and PACl as a function of Al dosage (Fig. 4). It was observed that the IOM species with higher MW were preferentially removed, and PACl exhibited more pronounced removal than that of AlCl₃. Quantitatively, the maximum removal of HMw, MMw, and LMw by AlCl₃ was 100% at 5.0 mg/L, 70.7% at 5.0 mg/L, and 49.4% at 7.0 mg/L. PACl at 2.0 mg/L contributed to the maximum removal of 100% for HMw, 76.8% for MMw, and 55.7% for LMw.

To further compare the removal efficiencies of these two coagulants, the IOM was ultra-filtered to IOM fractions with various MW, *i.e.*, > 100 kDa, 30–100 kDa, 5–30 kDa, and < 5 kDa, after which they were respectively treated by coagulation, and their removal efficiencies in terms of DOC and UV₂₅₄ are illustrated in Fig. 5. PACl was more effective than AlCl₃ at removing IOM as DOC, especially for the fractions of > 100 kDa and < 5 kDa (Fig. 5a). Among these fractions, the removal of the > 100 kDa fraction was highest, at 69.8% by AlCl₃ and 80.3% by PACl. It was noted that PACl exhibited no superiority regarding the removal of the 30–100 kDa fraction as compared

to AlCl₃. Additionally, PACl was not necessarily better than AlCl₃ with respect to UV₂₅₄ removal, and there was insignificant difference in the removal of 30–100 kDa and < 5 kDa fractions between them (Fig. 5b). Considering that AlCl₃ showed lower DOC removal for the < 5 kDa fraction, it was inferred that the IOM fraction with higher SUVA₂₅₄, *i.e.*, the ratio of UV₂₅₄ to DOC, was more easily removed by AlCl₃.

EEM analysis provided additional information about the removal of fluorescent substances derived from IOM fractions with different MW by AlCl₃ and PACl coagulation. For tyrosine-like, humic-like and dissolved microbial metabolites, both PACl and AlCl₃ achieved removal efficiency as high as 100% regardless of the MW. However, the removal of tryptophan-like aromatic proteins by Al coagulation was dependent on their MW (Appendix A Table S1). As for the removal of > 5 kDa IOM fractions, AlCl₃ coagulation contributed to lower fluorescence intensity of tryptophan-like aromatic proteins than PACl, especially for 30–100 and 5–30 kDa fractions. This was in accordance with a previous report that hydrophobic humic acids with higher MW were more easily
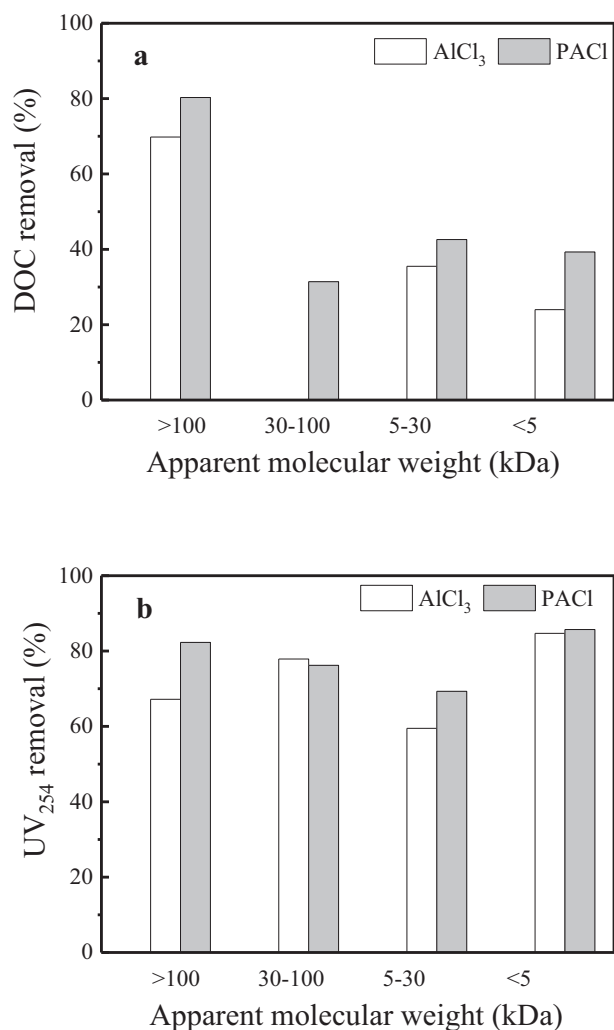
the A_{680} values were even much lower. This was possibly due to the irreversible association of some IOM compounds with the XRD resins (Henderson et al., 2008). UV_{254} and $SUVA_{254}$ are often indicative of the unsaturated C=C and C=O groups within aromatic organics, and these unsaturated organics were inferred to mainly exist in the HPI faction. HPO showed the highest intensity of both Peak P2 and Peak DM, which were related to the tryptophan-like aromatic proteins and the dissolved microbial metabolites, respectively. Henderson et al. (2008) also reported that IOM was dominated by hydrophobic proteins and hydrophilic polysaccharides.

2.3.2. Removal of IOM with different molecular polarity

The removal efficiency of IOM with different molecular polarity by $AlCl_3$ and PACl, as expressed by the removal of DOC and UV_{254}, is illustrated in Fig. 6. PACl showed a pronounced advantage with regard to the removal of HPO and HPI fractions. PACl achieved removal of 90.2% for HPO and 23.7% for HPI, whereas their removal by $AlCl_3$ was 83.7% and 8.7%, respectively. HPI was most difficult to remove by coagulation among these fractions. That PACl showed superiority in HPI removal is
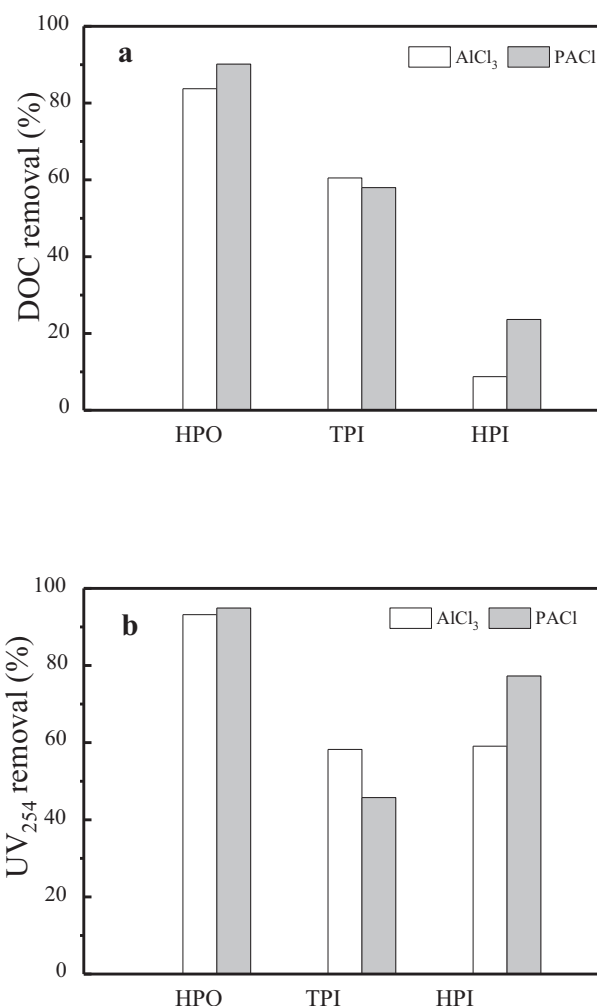
Fig. 5 – Removal of intracellular organic matter (IOM) fractions with MW of >100 k, 30–100 k, 5–30 k, and < 5 kDa in terms of (a) DOC and (b) UV_{254} by Al coagulation. DOC = 5.0 mg/L, Turbidity = 100 nephelometric turbidity units (NTU), Initial pH = 7.0.

removed by $AlCl_3$ (Shi et al., 2007). The superiority of PACl may be best illustrated by its high efficacy at removing the low MW fraction (<5 kDa), the removal of which was 40.5%, whereas that by $AlCl_3$ was as low as 15.9%.

2.3. Removal of IOM fractions with different molecular polarity

2.3.1. Characteristics of IOM with different molecular polarity

As shown in Appendix A Table S2, the factions of HPI, TPI, and HPO showed DOC of 9.23, 2.74, and 9.01 mg/L, and the contributive ratios were determined to be 44.0%, 13.1%, and 42.9%, respectively. In addition, the SUVA values of IOM were related to their molecular polarity characteristics. The highest $SUVA_{254}$ values were associated with HPI and were as high as 0.117 L/(mg·m), and this was 2.7 and 4.8 times the values of TPI and HPO, respectively. This was in accordance with a previous report (Henderson et al., 2008). The observed values of UV_{254} and $SUVA_{254}$ in these fractions were lower than those with different MW obtained by ultrafiltration (Table 1), and

Fig. 6 – Removal of IOM fractions of hydrophobic (HPO), transphilic (TPI), and hydrophilic (HPI) in terms of (a) DOC and (b) UV_{254} by Al coagulation. DOC = 5.0 mg/L, Turbidity = 100 nephelometric turbidity units (NTU), Initial pH = 7.0.

of practical importance in the treatment of algae-laden source water in view of the potential risks of IOM release.

Similar trends were observed for these IOM components in terms of their UV_{254} removal, except that the removal of TPI was the lowest in comparison to HPO and HPI (Fig. 6b). This may be attributed to its critically low UV_{254} value prior to dosing with Al salts (Appendix A Table S2). With regard to UV_{254}, the removal in the HPI fraction by $AlCl_3$ was 59.1% and that by PACl was 77.3%, and the observed removal was higher than that in terms of DOC (Fig. 6a). HPI fractions include different components, and this result indicated that the species with high $SUVA_{254}$ were removed preferentially by Al coagulation. Additionally, $AlCl_3$ contributed to higher TPI removal than PACl did, as indicated from the removal of both DOC and UV_{254}, and more significant superiority was observed for UV_{254}. The components within TPI with higher $SUVA_{254}$ were more effectively removed by $AlCl_3$.

The EEM spectra of HPI, TPI, and HPO are illustrated in Appendix A Fig. S7, and the hydrophobic tryptophan-like aromatic proteins were observed to be important components within these IOM fractions. $AlCl_3$ showed higher removal of this component within all three fractions of HPO, TPI, and HPI than PACl did (Appendix A Table S3). After coagulation by $AlCl_3$ and PACl, the intensity of the HPO aromatic proteins was observed to be 142.0 and 269.2 A.U., and similar trends were also observed for those within TP and HPI. Generally, $AlCl_3$ was more effective than PACl at removing the components with high $SUVA_{254}$ within TPI and the tryptophan-like aromatic proteins. Comparatively, PACl showed more significant removal of HPI and HPO as compared to $AlCl_3$. In considering the much higher contribution ratios of HPI and HPO within IOM (Appendix A Table S2), PACl was more effective for IOM removal.

2.4. The removal mechanism for IOM by Al coagulation

PACl is the most widely-used inorganic polymer coagulant in drinking water treatment. The main Al species within PACl is preformed Al polymer, i.e., Al_{13}, which shows higher positive charge and larger molecular diameter as compared to aluminum ions (Al^{3+}). It is widely accepted that PACl shows better coagulation efficiency in a wider pH range and at lower temperature than $AlCl_3$ does (Tang et al., 2015) owing to the higher efficacy of Al_{13} in terms of charge neutralization, bridging, adsorption, and sweeping (Duan and Gregory, 2003; Shi et al., 2007). In this study, the Al_b (i.e., Al_{13}) content within PACl was much higher than that within $AlCl_3$ (Table 1), and lower PACl doses were required to achieve isoelectric points (Appendix A Fig. S1).

However, PACl did not definitively show higher efficiency than $AlCl_3$ with regard to the removal of soluble organics. PACl showed superiority in the DOC removal of the >100 kDa and <5 kDa IOM fractions (Fig. 5a) and the HPO and HPI IOM fractions (Fig. 6a). Comparatively, $AlCl_3$ showed advantages in the removal of IOM species such as the TPI fraction and the hydrophobic tryptophan-like aromatic proteins. Our previous study also reported the higher efficiency of $AlCl_3$ than PACl in the treatment of eutrophic water, because of the combined effects of in situ Al_{13} formation and more significant pH depression involved in $AlCl_3$ coagulation (Hu et al., 2006). Additionally, the high MW and hydrophobic humic acids tended to form insoluble complexes with Al^{3+} and Al hydrolysis

products, and this effect also contributed to their higher removal efficiency (Shi et al., 2007).

Besides the effect of differences in Al species, the interactions between Al species and IOM fractions also played an important role. The values of differential log-transformed A_{254} ($DLnA_{254}$) and A_{350} ($DLnA_{350}$) were calculated according to the methods developed by Yan et al. (2013), and their correlation with the doses of PACl and $AlCl_3$ in the range of 0.05–0.5 mg/L as Al is illustrated in Appendix A Fig. S8. The $AlCl_3$ doses were positively correlated with the values of $DLnA_{254}$ and $DLnA_{350}$, with R^2 of 0.91 and 0.89, respectively. Comparatively, there was no correlation when PACl was introduced. While investigating the interactions between humic acid and Al species, the concentrations of NOM-Al complexes, as obtained from MINTEQ calculations, were positively correlated with the $DLnA_{350}$ values (Yan et al., 2013). It was inferred that the formation of Al-IOM complexes was involved in the removal of IOM by $AlCl_3$. This was also supported by the higher residual Al concentrations after $AlCl_3$ coagulation (in the range from 0.13 to 0.59 mg/L), which were twice those observed after PACl coagulation (Fig. 1c). The formation of Al-IOM complexes may also have occurred during PACl coagulation, but the extent was much lower. The stronger formation of Al-IOM complexes enables $AlCl_3$ to show better efficiency towards IOM fractions with high $SUVA_{254}$ (Fig. 2). The observed $SUVA_{254}$ was mainly ascribed to the aromaticity of IOM (Hoyer et al., 1987), and was effectively indicative of humic/fulvic type aromaticity, rather than the aromatic tryptophan-like proteins (Henderson et al., 2008). However, it was reported that PACl tended to remove the aromatic $C{=}C$ groups within HA better as compared to monomeric aluminum (Lin et al., 2014). This may be attributed to the fact that $SUVA_{254}$ corresponded to different species between IOM and humic acid.

$AlCl_3$ showed superiority with regard to the removal of tryptophan-like aromatic proteins (Appendix A Table S3). Upon being dosed, the aluminum ions tended to rapidly transform to different species of (1) monomeric and dimeric aluminum, (2) small polymeric aluminum (Al_3–Al_5 species), (3) median polymeric species (Al_6–Al_{10} species), (4) large polymeric species (Al_{11}–Al_{21} species), and (5) $Al(OH)_3$ amorphous flocs (Zhao et al., 2009), and the hydrolysis product distributions were highly dependent on pH. The proteins within IOM tended to form soluble complexes with Al salts and their hydrolysis intermediates (Ma et al., 2012b), which interfered with their further hydrolysis and precipitation thereafter. This adverse effect may be overcome by increasing the Al dose, in which case the aggregation and attachment of hydrolysis products was enhanced. The improved coagulant precipitation was beneficial to the removal of IOM by floc adsorption (Bernhardt et al., 1985; Jekel and Heinzmann, 1989).

In comparison to $AlCl_3$, PACl exhibits higher charge density and is more stable over a wide pH range, and these effects enable its better efficacy for charge neutralization, especially at relatively low doses. Additionally, the hydrolysis rate of Al_{13} was much lower than that of Al^{3+} during coagulation (Wang et al., 2004), and thus Al_{13} species benefited the adsorption and removal of negative IOM with low MW (Fig. 5). After charge neutralization, floc growth occurred owing to the attachment and aggregation of destabilized colloids, and Al_{13} polymer enabled more significant floc growth, which enhanced the removal of IOM by floc sweeping. However, the formation of complexes between Al_{13}

and IOM was much lower than that between Al^{3+} and IOM (Appendix A Fig. S8), and lower efficiency in the removal of $SUVA_{254}$ and tryptophan-like aromatic proteins was observed accordingly. Additionally, overdosed PACl with high charge density may affect the structure of organics greatly (Shi et al., 2007), and the dissolution of some high MW IOM such as pigment-like species as indicated by A_{680} may occur, inhibiting IOM removal (Fig. 2c). Furthermore, in the presence of ligands such as humic acid (Hiradate and Yamaguchi, 2003; Lin et al., 2014) and fluoride (He et al., 2016), Al_{13} polymer tended to decompose into small polymeric and monomeric Al. IOM might also dissolve the stable Al_{13} Keggin-structure and affect IOM removal thereafter. These results indicated that distinct reactions and species transformation mechanisms are involved in the coagulation of IOM by these two coagulants.

3. Conclusions

In the treatment of eutrophic algae-laden source water, the removal of IOM is important to minimize its adverse effects on water safety. IOM is composed of different fractions in terms of physiochemical characteristics such as molecular weight distribution and polarity, and this gives them different treatability in Al-based coagulation. On the other hand, PACl and AlCl₃ show different Al species distribution and coagulation mechanisms, and this complicates the IOM removal by coagulation. PACl, with higher ratio of Al_b, i.e., Al_{13} polymer with higher charge density, showed higher removal efficiency towards IOM than monomeric AlCl₃, and its superiority in the removal of low MW and hydrophilic IOM played a significant role. However, the formation of complexes between Al^{3+} and tryptophan-like proteins is more significant upon the introduction of AlCl₃, and this effect benefits the removal of tryptophan-like proteins. This study indicates that the interactions between Al species and IOM should be carefully evaluated to maximize IOM removal by Al coagulation, and to minimize its adverse effects on water safety as much as possible thereafter.

Acknowledgments

Appendix A. Supplementary data

Supplementary data to this article can be found online at https://doi.org/10.1016/j.jes.2018.05.011.

REFERENCES

Aktas, T.S., Takeda, F., Maruo, C., Fujibayashi, M., Nishimura, O., 2013. Comparison of four kinds of coagulants for the removal of picophytoplankton. Desalin. Water Treat. 51, 3547–3557.

Baresova, M., Naceradska, J., Kopecka, I., Pivokonsky, M., 2015. Coagulation mechanisms for removal of peptides and proteins produced by phytoplankton. Chem. List. 109, 98–104.

Becker, E.W., 1994. Microalgae: Biotechnology and Microbiology, Cambridge Studies in Biotechnology. Cambridge University Press, Cambridge (CB2 1RP, England, p. vii+293p).

Bernhardt, H., Hoyer, O., Schell, H., Lusse, B., 1985. Reaction-mechanisms involved in the influence of algogenic organic-matter on flocculation. Z. Wasser Abwasser Forsch. 18, 18–30.

Chen, W., Westerhoff, P., Leenheer, J.A., Booksh, K., 2003. Fluorescence excitation-emission matrix regional integration to quantify spectra for dissolved organic matter. Environ. Sci. Technol. 37, 5701–5710.

Chen, J.J., Yeh, H.H., Tseng, I.C., 2009. Effect of ozone and permanganate on algae coagulation removal—pilot and bench scale tests. Chemosphere 74, 840–846.

Cheng, W.P., Chi, F.H., 2003. Influence of eutrophication on the coagulation efficiency in reservoir water. Chemosphere 53, 773–778.

Chow, C.W.K., Fabris, R., Van Leeuwen, J., Wang, D., Drikas, M., 2008. Assessing natural organic matter treatability using high performance size exclusion chromatography. Environ. Sci. Technol. 42, 6683–6689.

Cory, R.M., Miller, M.P., McKnight, D.M., Guerard, J.J., Miller, P.L., 2010. Effect of instrument-specific response on the analysis of fulvic acid fluorescence spectra. Limnol. Oceanogr. Methods 8, 67–78.

Duan, J.M., Gregory, J., 2003. Coagulation by hydrolysing metal salts. Adv. Colloid Interf. Sci. 100, 475–502.

Duan, S.X., Xu, H., Xiao, F., Wang, D.S., Ye, C.Q., Jiao, R.Y., Liu, Y.J., 2014. Effects of Al species on coagulation efficiency, residual Al and floc properties in surface water treatment. Colloids Surf. A Physicochem. Eng. Asp. 459, 14–21.

Edzwald, J.K., 1993. Coagulation in drinking-water treatment-particles, organics and coagulants. Water Sci. Technol. 27, 21–35.

Elcik, H., Cakmakci, M., Ozkaya, B., 2016. The fouling effects of microalgal cells on crossflow membrane filtration. J. Membr. Sci. 499, 116–125.

Ewerts, H., Barnard, S., Swanepoel, A., Du Preez, H.H., Van Vuuren, S.J., 2014. Strategies of coagulant optimisation to improve the removal of turbidity and Ceratium hirundinella cells during conventional drinking water purification. Water Sci. Technol. Water Supply 14, 820–828.

Fang, J.Y., Yang, X., Ma, J., Shang, C., Zhao, Q.A., 2010. Characterization of algal organic matter and formation of DBPs from chlor(am) ination. Water Res. 44, 5897–5906.

Gone, D.L., Seidel, J.-L., Batiot, C., Bamory, K., Ligban, R., Biemi, J., 2009. Using fluorescence spectroscopy EEM to evaluate the efficiency of organic matter removal during coagulation–flocculation of a tropical surface water (Agbo reservoir). J. Hazard. Mater. 172, 693–699.

Gonzalez-Torres, A., Putnam, J., Jefferson, B., Stuetz, R.M., Henderson, R.K., 2014. Examination of the physical properties of Microcystis aeruginosa flocs produced on coagulation with metal salts. Water Res. 60, 197–209.

Hammes, F., Meylan, S., Salhi, E., Koester, O., Egli, T., Von Gunten, U., 2007. Formation of assimilable organic carbon (AOC) and specific natural organic matter (NOM) fractions during ozonation of phytoplankton. Water Res. 41, 1447–1454.

He, Z., Lan, H.C., Gong, W.X., Liu, R.P., Gao, Y.P., Liu, H.J., Qu, J.H., 2016. Coagulation behaviors of aluminum salts towards fluoride: significance of aluminum speciation and transformation. Sep. Purif. Technol. 165, 137–144.

Henderson, R.K., Baker, A., Parsons, S.A., Jefferson, B., 2008. Characterisation of algogenic organic matter extracted from cyanobacteria, green algae and diatoms. Water Res. 42, 3435–3445.

Her, N., Amy, G., Park, H.R., Song, M., 2004. Characterizing algogenic organic matter (AOM) and evaluating associated NF membrane fouling. Water Res. 38, 1427–1438.

Hiradate, S., Yamaguchi, N.U., 2003. Chemical species of Al reacting with soil humic acids. J. Inorg. Biochem. 97, 26–31.

Hoyer, O., Bernhardt, H., Lusse, B., 1987. The effect of ozonation on the impairment of flocculation by algogenic organic-matter. Z. Wasser Abwasser Forsch. 20, 123–131.

Hu, C.Z., Liu, H.J., Qu, J.H., Wang, D.S., Ru, J., 2006. Coagulation behavior of aluminum salts in eutrophic water: significance of Al-13 species and pH control. Environ. Sci. Technol. 40, 325–331.

Jekel, M.R., Heinzmann, B., 1989. Residual aluminium in drinking water treatment. J. Water Supply Res Technol. 38, 281–288.

Jiao, R., Fabris, R., Chow, C.W.K., Drikas, M., Van Leeuwen, J., Wang, D., 2016. Roles of coagulant species and mechanisms on floc characteristics and filterability. Chemosphere 150, 211–218.

Li, L., Gao, N.Y., Deng, Y., Yao, J.J., Zhang, K.J., 2012. Characterization of intracellular & extracellular algae organic matters (AOM) of microcystic aeruginosa and formation of AOM-associated disinfection byproducts and odor & taste compounds. Water Res. 46, 1233–1240.

Lin, J.L., Huang, C., Dempsey, B.A., Hu, J.Y., 2014. Fate of hydrolyzed Al species in humic acid coagulation. Water Res. 56, 314–324.

Ma, M., Liu, R.P., Liu, H.J., Qu, J.H., 2012a. Chlorination of Microcystis aeruginosa suspension: cell lysis, toxin release and degradation. J. Hazard. Mater. 217-218, 279–285.

Ma, M., Liu, R.P., Liu, H.J., Qu, J.H., Jefferson, W., 2012b. Effects and mechanisms of pre-chlorination on Microcystis aeruginosa removal by alum coagulation: significance of the released intracellular organic matter. Sep. Purif. Technol. 86, 19–25.

Matilainen, A., Gjessing, E.T., Lahtinen, T., Hed, L., Bhatnagar, A., Sillanpää, M., 2011. An overview of the methods used in the characterisation of natural organic matter (NOM) in relation to drinking water treatment. Chemosphere 83, 1431–1442.

Nicholls, K.H., Dillon, P.J., 1978. Evaluation of phosphorus–chlorophyll–phytoplankton relationships for lakes. Int. Rev. Gesamten Hydrobiol. 63, 141–154.

Paralkar, A., Edzwald, J.K., 1996. Effect of ozone on EOM and coagulation. J. Am. Water Works Assoc. 88, 143–154.

Pivokonsky, M., Kloucek, O., Pivokonska, L., 2006. Evaluation of the production, composition and aluminum and iron complexation of algogenic organic matter. Water Res. 40, 3045–3052.

Qu, F.S., Liang, H., He, J.G., Ma, J., Wang, Z.Z., Yu, H.R., Li, G.B., 2012. Characterization of dissolved extracellular organic matter (dEOM) and bound extracellular organic matter (bEOM) of Microcystis aeruginosa and their impacts on UF membrane fouling. Water Res. 46, 2881–2890.

Shi, B.Y., Wei, Q.S., Wang, D.S., Zhu, Z., Tang, H.X., 2007. Coagulation of humic acid: the performance of preformed and non-preformed Al species. Colloids Surf. A Physicochem. Eng. Asp. 296, 141–148.

Song, B., Zhang, C., Zeng, G., Gong, J., Chang, Y., Jiang, Y., 2016. Antibacterial properties and mechanism of graphene oxide-silver nanocomposites as bactericidal agents for water disinfection. Arch. Biochem. Biophys. 604, 167–176.

Takaara, T., Sano, D., Konno, H., Omura, T., 2007. Cellular proteins of Microcystis aeruginosa inhibiting coagulation with polyaluminum chloride. Water Res. 41, 1653–1658.

Takaara, T., Sano, D., Masago, Y., Omura, T., 2010. Surface-retained organic matter of Microcystis aeruginosa inhibiting coagulation with polyaluminum chloride in drinking water treatment. Water Res. 44, 3781–3786.

Tang, H.X., Xiao, F., Wang, D.S., 2015. Speciation, stability, and coagulation mechanisms of hydroxyl aluminum clusters formed by PACl and alum: a critical review. Adv. Colloid Interf. Sci. 226, 78–85.

Wang, D.S., Sun, W., Xu, Y., Tang, H.X., Gregory, J., 2004. Speciation stability of inorganic polymer flocculant-PACl. Colloids Surf. A Physicochem. Eng. Asp. 243, 1–10.

Watson, S.B., Monis, P., Baker, P., Giglio, S., 2016. Biochemistry and genetics of taste- and odor-producing cyanobacteria. Harmful Algae 54, 112–127.

Yan, M., Wang, D., Korshin, G.V., Benedetti, M.F., 2013. Quantifying metal ions binding onto dissolved organic matter using log-transformed absorbance spectra. Water Res. 47, 2603–2611.

Zamyadi, A., Macleod, S.L., Fan, Y., Mcquaid, N., Dorner, S., Sauve, S., Prevost, M., 2012. Toxic cyanobacterial breakthrough and accumulation in a drinking water plant: a monitoring and treatment challenge. Water Res. 46, 1511–1523.

Zhao, H., Hu, C.Z., Liu, H.J., Zhao, X., Qu, J.H., 2008. Role of aluminum speciation in the removal of disinfection byproduct precursors by a coagulation process. Environ. Sci. Technol. 42, 5752–5758.

Zhao, H., Liu, H.J., Qu, J.H., 2009. Effect of pH on the aluminum salts hydrolysis during coagulation process: formation and decomposition of polymeric aluminum species. J. Colloid Interface Sci. 330, 105–112.